

# “Analysis of CNT-Si Heterojunction Solar Cells”

By

Md. Roqibul Hasan

Lasker Aminul Islam



Submitted to the


Department of Electrical & Electronic Engineering

East West University

In partial fulfillment of the requirements for the degree of  
Bachelor of Science in Electrical & Electronic Engineering

(B.Sc in EEE)

Summer, 2011

  
02.10.2011

Thesis Advisor

Dr. Anisul Haque



  
02.10.2011

Chairperson


Dr. Anisul Haque

# ABSTRACT

In this thesis heterojunction formation of carbon nanotube (CNT) with silicon (Si) is studied to design new kind of solar cells. The nanoscale structure, high mobility and high physical and electrical properties of CNT can be used to improve the efficiency of solar cell. Here we analyzed i-n (CNT in i-side and Si in n-side) heterojunction solar cells. By varying the diameter of carbon nanotube (CNT), the bandgap can be varied according to our desired value. Here we vary the diameter of CNT around 1nm to check the characteristics of this solar cell. To form heterojunction of CNT with Si we assumed CNT as intrinsic and an equation has been developed to find the band diagram. We calculated the short circuit current density ( $J_{sc}$ ) by using the data for terrestrial solar irradiance with Air Mass 1.5. Calculation has been made assuming solar cell is ideal. To calculate Fill Factor and Efficiency for different diameter of CNTs, we have calculated the total current density and the open circuit voltage. MATLAB software has been used for calculation. P-V curve is also plotted to find the maximum power point and from that fill factor (FF) and efficiency ( $\eta$ ) is calculated. In this paper we show different open circuit voltage, short circuit current, fill factor and efficiency for different diameter of CNT. All the parameters decrease with the decrement of diameters of CNT. In our model the best efficiency is 22.663% for of 1.92nm diameter of CNT. We compared the efficiency variation for different diameters of CNT and proposed a range of CNT diameter to design the CNT-Si heterojunction solar cells, in which range efficiency remains stable and higher.

# APPROVAL

The thesis titled “Analysis of CNT-Si heterojunction solar cells” submitted by **Md. Roqibul Hasan (2007-2-80-030)** and **Lasker Aminul Islam (2007-2-80-027)**, session summer, 2011, has been accepted satisfactory in partial fulfillment of the requirement of the degree of Bachelor of Science in Electrical and Electronic Engineering on August, 2011.

 02.10.2011

Dr. Anisul Haque

Professor and Chairperson

Department of Electrical and Electronic Engineering

East West University

Dhaka-1212, Bangladesh.

# AUTHORIZATION PAGE

We hereby declare that we are the sole authors of the thesis. We authorize East West University to lend this thesis to other institution or individuals for the purpose of scholarly research.

R. Hasan.

(Md. Roqibul Hasan)

Aminul

(Lasker Aminul Islam)

We further authorize East West University to reproduce this thesis by photocopy or other means, in total or in part, at the request of other institutions or individuals for purpose of scholarly research.

R. Hasan.

(Md. Roqibul Hasan)

Aminul

(Lasker Aminul Islam)

# TABLE OF CONTENTS

ABSTRACT.....	i
ACKNOWLEDGEMENTS .....	ii
APPROVAL .....	iii
AUTHORIZATION PAGE .....	iv
TABLE OF CONTENTS.....	v
LIST OF FIGURES.....	vii
LIST OF TABLES.....	viii
CHAPTER 1.....	1
<b>Introduction</b> .....	1
1.1 Heterojunctions.....	2
1.2 Literature review.....	4
1.3 Why use CNT in solar cell .....	7
1.4 Objective .....	8
CHAPTER 2.....	9
<b>CNT-Si Heterojunction</b> .....	9
2.1 Model .....	9
2.2 Equations developed for the proposed model.....	10
CHAPTER 3.....	14
<b>CNT-Si Heterojunction Solar Cells</b> .....	14
3.1 Solar Cell Basics.....	14
3.2 Solar Spectrum .....	16
3.3 Short Circuit Current Density ( $J_{sc}$ ).....	17
3.4 J-V Characteristics.....	19
3.5 Open Circuit Voltage ( $V_{OC}$ ) .....	20
3.6 Efficiency .....	21
CHAPTER 4.....	24
<b>4.1 Results and Discussion</b> .....	24

<b>CHAPTER 5</b> .....	<b>32</b>
<b>Conclusions</b> .....	<b>32</b>
5.1 Summary .....	32
5.2 Suggestion for future work.....	33
<b>References</b> .....	<b>34</b>



# LIST OF FIGURES

Figure 01.1: Heterojunction formation (a) Before contact (b) After contact. ....	3
Figure 02.1: Electron and hole separation in CNT-Si heterojunction. ....	9
Figure 02.2: Band diagram of CNT-Si heterojunction model .....	12
Figure 03.1: The photovoltaic effect in a solar cell .....	14
Figure 03.2 : p-n junction solar cell with resistive load. ....	15
Figure 03.3: Wavelength vs spectral irradiance at AM 1.5 and showing the absorption re- gion of CNT and Si separately.....	16
Figure 03.4: Equivalent circuit of ideal solar cell.....	20
Figure 03.5: J-V and P-V curves showing $V_{oc}$ , $J_{sc}$ , maximum power point, $J_m$ and $V_m$ ....	22
Figure 04.1: Energy band diagram of CNT-Si heterojunction for 1.92nm diameter of CNT .....	24
Figure 04.2: The J-V and P-V curves for 1.92nm diameter of CNT.....	25
Figure 04.3: Energy band diagram of CNT-Si heterojunction for 1.45nm diameter of CNT. ....	25
Figure 04.4: The J-V and P-V curves for 1.45nm diameter of CNT.....	26
Figure 04.5: Energy band diagram of CNT-Si heterojunction for 0.98nm diameter of CNT. ....	26
Figure 04.6: The J-V and P-V curves for 0.98nm diameter of CNT.....	27
Figure 04.7: The plot of diameter of CNT vs efficiency. ....	31

# LIST OF TABLES

Table 01: The current density and open circuit voltage with different diameters of CNT.....	29
Table 02: The $P_{mp}$ , $V_{mp}$ , $J_{mp}$ , FF and $\eta$ with different diameters of CNT.....	30



# CHAPTER 1

## Introduction

Limited conventional resources of energy production such as fossil and nuclear fuels and the association of their negative environmental effect forced the researchers to introduce renewable energy resources that are environmentally friendly. The conversion of sunlight into electricity using photovoltaics (PV) is a very attractive way to produce renewable energy. At the very beginning of the solar cell research, introduction of the new kind of solar cell was the major issue. But recently cost effectiveness as well as efficiency increment has become a major research goal of the researchers around the world. Recently researchers have introduced CNT as a potential material to improve efficiency and cost effectiveness and research is still on going to improve the efficiency. A strong optoelectronic property of the CNT makes it a strong candidate of basic building block of PV devices. On the other hand about 85% solar cells are based on Si substrate. Research shows that CNT forms heterojunctions with Si to form solar cells and convert photon into electricity very efficiently.

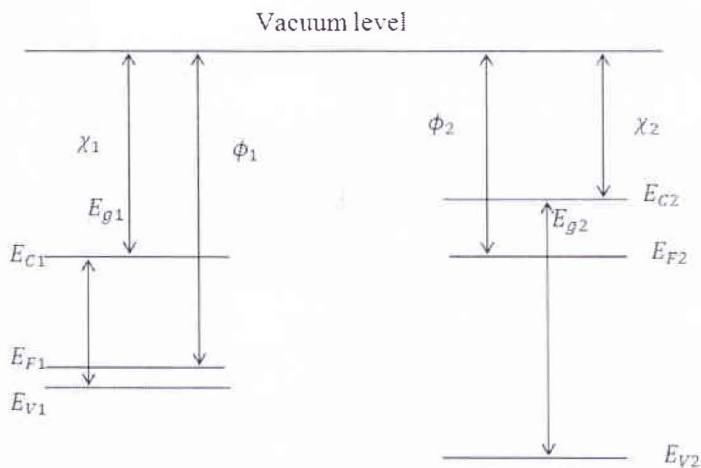


## 1.1 Heterojunctions

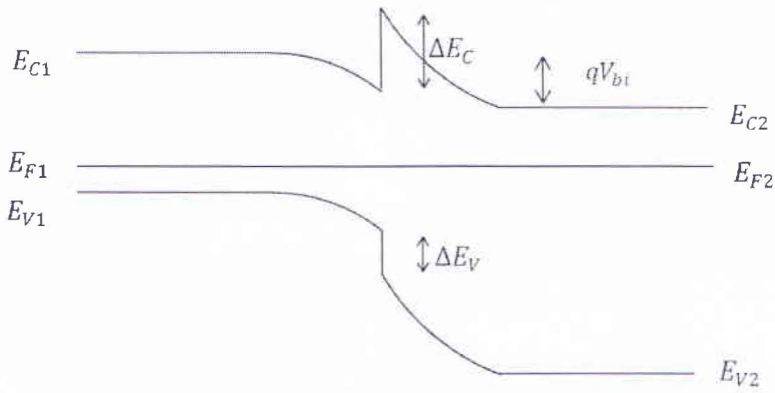
A heterojunction is formed when two semiconductors with different bandgaps are brought together. Heterojunctions form essential constituents of many electronic and optoelectronic devices. Anderson rule is mostly use to make a model of heterojunction between two materials.

The two semiconductors are assumed to have different bandgaps,  $E_g$ , different permittivities,  $\epsilon_s$ , different work function,  $\phi$  and different electron affinities,  $\chi$ . Work function and electron affinity are defined as energy required to remove an electron from the Fermi level  $E_F$  and from the bottom of the conduction band  $E_C$ , respectively, to a position just outside the material (vacuum level).

For example, let's assume bandgap of material 2 is greater than bandgap of material 1 ( $E_{g2} > E_{g1}$ ). The band diagram of the ideal heterojunction will form like Figure 01.1.



(a)



(b)

Figure 01.1: Heterojunction formation (a) Before contact (b) After contact.

Here,

$\chi_1$  and  $\chi_2$  are the electron affinities,  $\phi_1$  and  $\phi_2$  are the work functions,  $E_{C1}$  and  $E_{C2}$  are the conduction bands,  $E_{V1}$  and  $E_{V2}$  are the valence bands,  $E_{g1}$  and  $E_{g2}$  are the bandgaps of p-type and n-type material respectively.  $\Delta E_C$  and  $\Delta E_V$  are the band offset of conduction and valence band respectively.  $\Delta E_{F1}$  and  $\Delta E_{F2}$  are the distance from the Fermi level to the conduction band of p-type and n-type material respectively.



According to Anderson model, the conduction band offset,  $\Delta E_c$  is given by,

$$\Delta E_c = \chi_1 - \chi_2 = \Delta\chi \quad (1.1)$$

Then the valence band offset is given by,

$$\Delta E_v = (E_{g_1} - E_{g_2}) - (\chi_1 - \chi_2) = \Delta E_g - \Delta\chi \quad (1.2)$$

Built in potential is given by,

$$qv_{bi} = \phi_1 - \phi_2 \quad (1.3)$$

Then the corresponding depletion layer thicknesses in the p-region and n-region can be found from solving the poissons equation given as,

$$\frac{d^2\phi}{dx^2} = -\frac{\rho}{\epsilon} \quad (1.4)$$

## 1.2 Literature review

Since the introduction of photovoltaic (PV) effect by Bequerral in 1839, this technology has come a long way. Since the early 1990's a lot of researchs has been carried out on solar cells <sup>[1]</sup>. Despite different PV cell technologies being explored, over 85% of the current production is based on the well-established silicon wafer technology.

The efficiency of most commercially available solar cells are about 15%-20% <sup>[2]</sup> even though the theoretical calculation shows 30% efficiency. Thus novel structured silicon solar cells with high efficiency are certainly of major importance for PV technology.

Recently, there have been a series of investigations on Carbon Nanotubes (CNTs) as a potential material that can be used in solar cells and other PV applications <sup>[3-9]</sup>. This means that CNT is a material that has already begun its interaction with Si, which indicates that there is a strong probability of succeeding in integrating CNT into solar cell technology.

In 2007 Yi Jia et.al. reported their work, where they fabricated thin-film solar cells with double-walled carbon nanotubes (DWNT) as energy conversion materials <sup>[3]</sup>. Here nanotubes serve as both photogenerated sites and charge carrier collection/transport layer. To favor charge separation and extract electrons (through n-Si) and holes (through nanotubes) they create high-density p-n heterojunctions between nanotubes and n-Si. The large carrier density and high mobility of DWNTs ensure much enhanced current density and power efficiency of solar cells compared to extensively studied polymer-nanotube composition structures. They achieved about 1% efficiency with this solar cell.

Yi Jia et.al. improved their cell efficiencies to about 5-7%, reported in 2008 <sup>[4]</sup>. In this work they used chemical vapor deposition (CVD) to grow spiderweb-like DWNT films in which nanotubes are highly interconnected. Where as in their previous work they achieved 1% cell efficiency, they deposited vertical nanotube arrays directly on silicon substrates to form nanotube-Si heterojunction solar cell.

Li. et.al. reported solar cell based on high-density p-n Heterojunction between single wall carbon nanotubes (SWCNTs) and a n-type silicon wafer <sup>[5]</sup>. In their model they have got more than 45% conversion efficiency through adjusting the Fermi level and increasing the carrier concentration and mobility with chemical modification of the SWCNT coating films. Electron-hole pairs are optically excited in the numerous heterojunctions formed between SWCNTs thin coating and n-type silicon substrate.

In 2010, another research group <sup>[6]</sup> reported photovoltaic devices based on SWNTs and n-silicon heterojunctions fabricated by a spray deposition process. They provide direct evidence that nanotubes serve as an active photosensing material involved directly in the photon absorption process as well as contributing to charge separation, transport and collection.

Zhang et.al reported in 2010 <sup>[7]</sup> that, they demonstrated carbon nanotube network on Si solar cell for photovoltaic enhancement. Single walled carbon nanotube (SWNT) networks were directly assembled onto the surface of n-p junction silicon solar cell for trapping incident photons and assisting electronic transportation at the interface of silicon solar cells. They have got 3.92% higher efficiency with assembling SWNT than that of silicon cell without SWNT.

Finally in 2011 Yi Jia et.al. again reported <sup>[8]</sup> their improved efficiency. This time they improved their efficiency from 7% to 13.8% by Silicon-Carbon Nanotube Hetrojunction Solar Cells by Acid Doping.

### 1.3 Why use CNT in solar cell

The 1D nanoscale structure, high mobility, and excellent physical and electronic properties of carbon nanotubes offer great promise in the development of high-efficiency solar cells <sup>[3]</sup>. Using CNT with solar cells, it creates multiple heterojunctions with Si based solar cells, adds more band gaps, which enables the solar cells to capture a wider spectrum of incident radiation.

On the other hand CNTs are highly transparent that allows them to replace glass layer due to their excellent conducting capability. CNTs can be combined with silicon to form heterojunction solar cells with modest efficiencies and high air stability. CNTs can be simply coated onto silicon wafers to form heterojunction solar cells. The manufacturing process is simple and scalable <sup>[4]</sup> and it does not require to separate metallic and semiconducting nanotubes.

In CNT-Si heterojunction solar cells CNT serves as an active photosensing material involved directly in the photon absorption process as well as contributing to charge separation, transport and collection.

CNTs have high carrier mobility and can be interconnected into two-dimensional networks with tunable electrical and optical properties <sup>[9]</sup>. Si-CNT structure holds several advantages and potentially could lead to low-cost and high-efficiency solar cells compared with p-n junction Si modules.

## 1.4 Objective

The objective of this thesis is to analyze the CNT-Si heterojunction solar cells. A model of i-n heterojunction to study the band diagram of CNT-Si heterojunction and observe the band formation for different diameters of CNT will be developed. In this model semiconducting CNT is used because it is easy to change the bandgap by changing only diameter of CNT. The main purpose of changing of diameter of CNT is to ensure more efficient absorption of photons. The J-V and P-V characteristic will also be analyzed to calculate the efficiency of the solar cell and to compare the efficiency for different diameters of CNT. We develop MATLAB code to analyze the behavior of heterojunction between CNT-Si. Short circuit current density for both regions will be found by integrating the appropriate region of photon energy that a i-n heterojunction solar cell can absorb. Quantum Efficiency (QE) will be included in the calculation of the short circuit current density. Other solar cells parameters will be calculated to compare the efficiency of the solar cells for different diameter of the CNT. It is expected to propose a better range of CNT diameter to design better efficiency CNT-Si heterojunction solar cells.





# CHAPTER 2

## CNT-Si Heterojunction

### 2.1 Model

Heterojunction formation of CNT with silicon (Si) has been analyzed. Assuming CNT is intrinsic type material and Si is n-type material heterojunction is formed. For simplicity of calculation we assumed that band bending in intrinsic type CNT is linear and calculation is made according to the following procedure. Electron and hole separation of CNT-Si heterojunction is shown in figure 02.1.

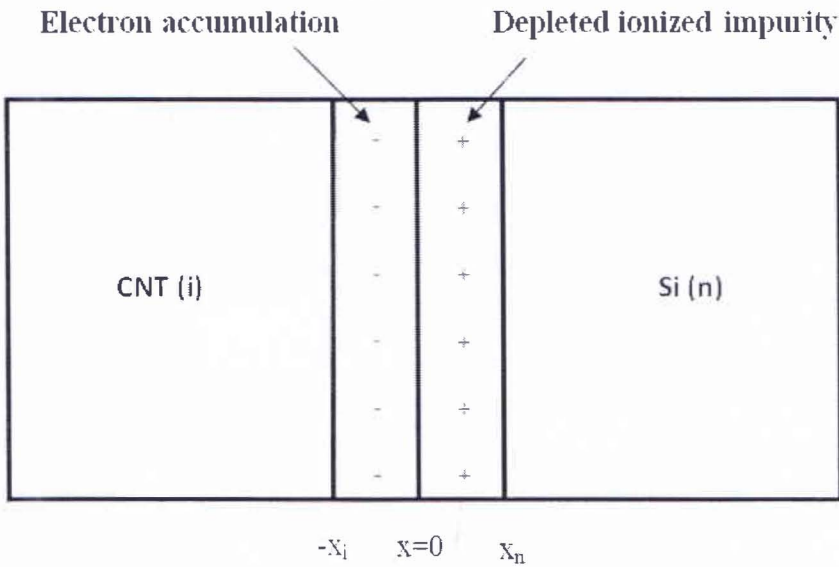


Figure 02.1: Electron and hole separation in CNT-Si heterojunction.

## 2.2 Equations developed for the proposed model

We calculated the excess electron of intrinsic CNT by integrating accumulated electrons in the range  $-x_i$  to 0. So the excess electron per unit area of accumulation region becomes,

$$n_s = \int_{x=-x_i}^{x=0} n(x) dx \quad (2.1)$$

Where,  $n(x)$  is the accumulation electron concentration in the range of  $-x_i$  to 0.

$$n(x) = n_i e^{\frac{\Phi(x)}{\Phi_t}} \quad (2.2)$$

Here,

$n_i$  = Intrinsic carrier concentration in intrinsic CNT region.

$\Phi(x)$  = Band bending in intrinsic CNT region.

$\Phi_t$  = Thermal voltage, ( $\frac{k_B T}{q} = 0.026$  V at room temperature).

$\Phi(x)$  is assumed to vary linearly within the accumulation region, using boundary condition,  $\Phi(-x_i) = 0$ ,  $\Phi(x)$  can be expressed as,

$$\Phi(x) = \Phi_i \left( 1 + \frac{x}{x_i} \right) \quad (2.3)$$

Here,

$\Phi_i$  is the barrier height of the intrinsic region shown in Figure 02.2.

So the equation of excess electrons becomes

$$n_s = \int_{x=-x_i}^{x=0} n_i e^{\frac{\phi_i}{\phi_t} \left(1 + \frac{x}{x_i}\right)} dx \quad (2.4)$$

By integrating the equation (2.4) we found the total excess electron of the intrinsic region,

$$n_s = n_i \frac{\phi_i}{\phi_t} \left[ e^{\frac{\phi_i}{\phi_t}} - 1 \right] \quad (2.5)$$

Poissons equation is solved to calculate the distance that the depletion region extends into the n-type Si material,  $x_n$

$$x_n = \sqrt{\frac{2\phi_d \epsilon_{Si}}{q N_d}} \quad (2.6)$$

Here,

$\phi_d$  = Barrier height of n-type Si region.

$\epsilon_{Si}$  = Permittivity of Silicon.

$N_d$  = Donor concentration ( $cm^{-3}$ ).

$q$  = Electron charge.

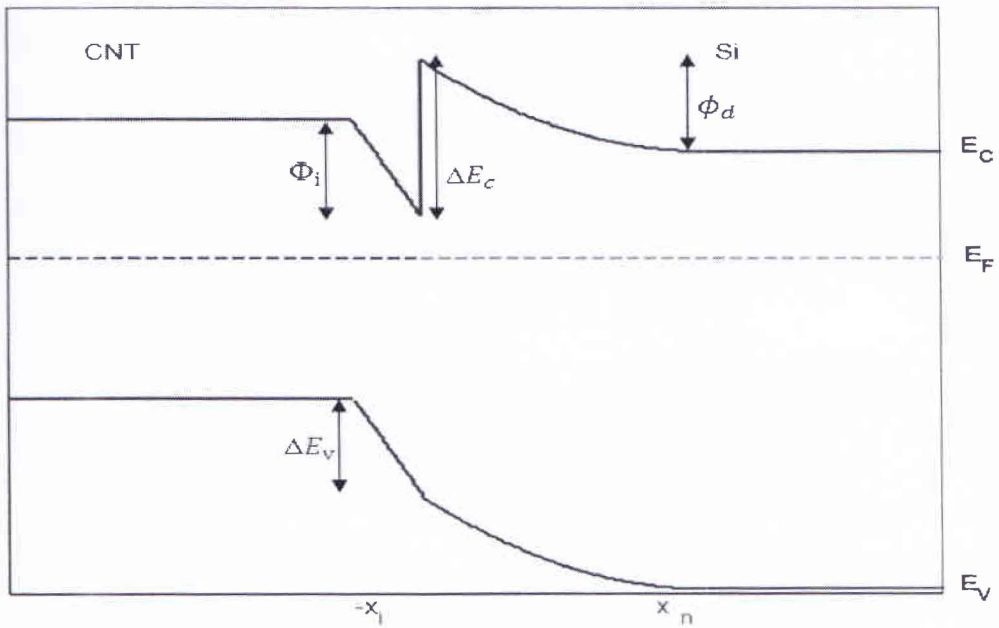


Figure 02.2: Band diagram of CNT-Si heterojunction model.

From the physics of heterojunction band diagram built voltage,  $v_{bi}$  can be expressed as,

$$v_{bi} = -\phi_i + \Delta E_c - \phi_d \quad (2.7)$$

Charge equality condition of accumulation and depletion region can be expressed as,

$$n_s = N_d x_n \quad (2.8)$$

Rearranging equation (2.7) we can write,

$$\phi_i + \phi_d = \Delta E_c - v_{bi} \quad (2.9)$$

From equation (2.8) we found,

$$n_i \frac{\phi_i}{\phi_t} \left[ e^{\frac{\phi_i}{\phi_t}} - 1 \right] - \sqrt{\frac{2\phi_d N_d \epsilon_{Si}}{q}} = 0 \quad (2.10)$$

So far  $\phi_i$  and  $\phi_d$  are the unknown parameters of equations (2.9) and (2.10). By solving equation (2.9) and equation (2.10) in MATLAB using numerical analysis, value of  $\phi_i$  and  $\phi_d$  can be found.

Electric flux density at just right side of  $x=0$  is equal to electric flux density at just left side of the  $x=0$  which can be mathematically expressed as,

$$\epsilon_{CNT} E(0^-) = \epsilon_{Si} E(0^+) \quad (2.11)$$

Here,  $E(0^-)$  is electric field at just left side of  $x=0$ , which is found by differentiating equation (2.3) at  $x=0$ . Which yields,

$$E(0^-) = -\frac{\phi_i}{x_i} \quad (2.12)$$

And  $E(0^+)$  is the electric field at just right side of the  $x=0$ , which can be found by differentiating the band bending equation of n-type region at  $x=0$ . We found the band bending equation of n-type region by solving poissons equation as,

$$\phi(x) = \frac{q N_d}{\epsilon_{Si}} \left[ x x_n - \frac{x^2}{2} \right] \quad (2.13)$$

So the electric field  $E(0^+)$  becomes,

$$E(0^+) = -\frac{q N_d x_n}{\epsilon_{Si}} \quad (2.14)$$

So from equation (2.3),

$$x_i = \frac{\epsilon_{CNT} \phi_i}{q N_d x_n} \quad (2.15)$$

# CHAPTER 3

## CNT-Si Heterojunction Solar Cells

### 3.1 Solar Cell Basics

Solar cell directly converts light energy to electrical energy and it produces current and voltage to generate electric power. Light is made up of packets of energy, called photons. The energy of the photons excite electrons up to higher energy levels where they are free to move. Normally, when light is absorbed by matter, photons are given up to excite electrons to higher energy states within the material, but the excited electrons quickly relax back to their ground state <sup>[10]</sup>. In a photovoltaic device (semiconductor) a built-in asymmetry pulls the excited electrons away before they can relax, and feeds them to an external circuit. The energy of the excited electrons generates a potential difference or electromotive force (e.m.f.). This force drives the electrons through a load in the external circuit to do electrical work. Figure 03.1 shows the photovoltaic effect in a solar cell. This PV cells are made of at least two layers of semi-conductor material.

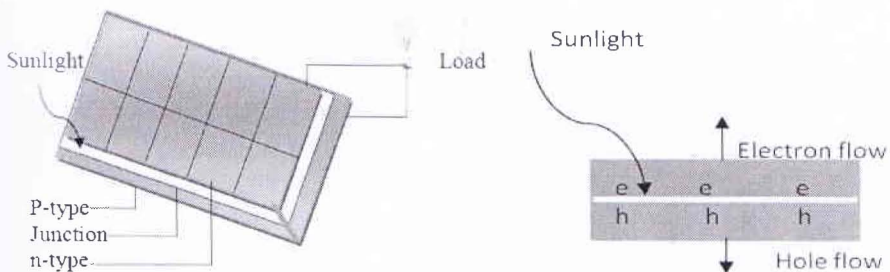


Figure 03.1: The Photovoltaic effect in a solar cell.

When light hits the cell, all photons of the light are not absorbed by the material. If the energy of photon is less than the bandgap (energy) of the material of the solar cell, that photon cannot be absorbed by the material of the solar cell. That photon can be absorbed by the material, whose energy is equal or greater than the bandgap (energy). So certain wavelengths of light are able to ionize the atoms in the material. Then an internal field produced by the junction separates some of the positive charges (holes) from the negative charges (electrons) within the photovoltaic device. This generated electron hole pair creates electricity. The generated electrons are collected by the electrode connected to the junction and serve the power to the load.

Figure 03.2 shows a solar cell circuit with resistive load <sup>[11]</sup>. Here incident photon illumination can create electron-hole pairs in the space charge region that will be swept out producing the photocurrent  $I_L$  in the reverse -bias direction. The photocurrent  $I_L$  produces a voltage drop across the resistive load which forward biases the p-n junction. The forward bias voltage produces a forward bias current  $I_F$  as indicated in the Figure 03.2. The photocurrent is always in the reverse-bias direction and the net solar cell current is also in the reverse bias direction <sup>[11]</sup>.

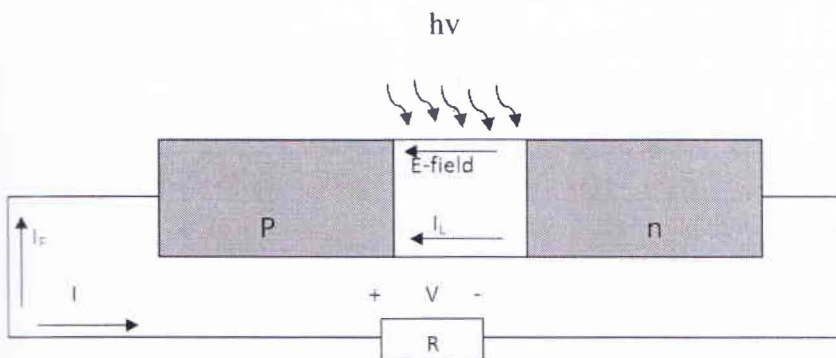
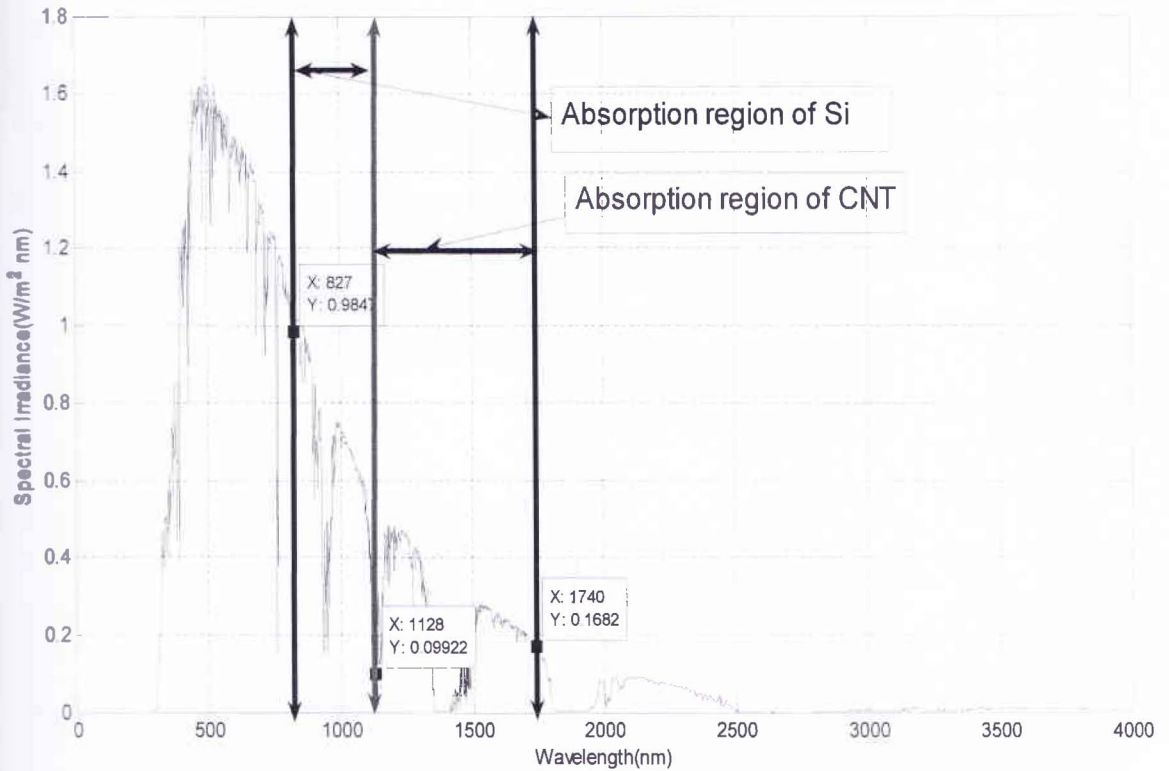


Figure 03.2: p-n junction solar cell with resistive load.

### 3.2 Solar Spectrum

The solar spectrum changes throughout the day and with location. Standard reference spectra are defined to allow the performance comparison of photovoltaic devices from different manufacturers and research laboratories. The air mass 1.5 (AM1.5) global spectrum is designed for flat plate modules and has an integrated power of 100 mW/cm<sup>2</sup>. Figure 03.3 shows solar spectrum at AM 1.5 and showing the absorption region of CNT and Si separately.



**Figure 03.3:** Wavelength vs spectral irradiance at AM 1.5 and showing the absorption region of CNT and Si separately.



### 3.3 Short Circuit Current Density ( $J_{sc}$ )

Short **circuit** current density is the current per unit area under the illumination of sunlight.

Short **circuit** current density can be written as,

$$J_{sc} = \int_{\lambda_l}^{\lambda_h} P(\lambda)QE(\lambda)d(\lambda) \quad (3.1)$$

Here,

$\lambda$  = **Wavelength** of the photon (nm).

$P(\lambda)$  = Number of photon/  $m^2$ sec.

$QE(\lambda)$  = Quantum efficiency.

$\lambda_l$  and  $\lambda_h$  are the lower and higher limits of the photon wave length to be integrated to find **the** current density of particular range of solar spectrum.

$P(\lambda)$  can be derived as equation (3.2),

$$P(\lambda) = \frac{\lambda^2 F}{hc} \quad (3.2)$$

Here,

$F$  = **Spectral irradiance** ( $W/m^2nm$ ).

$h$  = **Plank's** constant.

$c$  = **Speed** of light (Constant).



Quantum efficiency (Q.E.) is a measurement of how efficiently electron-hole pairs are generated in PV devices by the incident of photons. It may be given either as a function of wavelength or as energy. If all photon energies are converted into electrical energy the quantum efficiency is unity. The quantum efficiency for photons with energy below the band gap is zero.

Q.E. can be defined as the ratio between the materials bandgap energy in which photons are absorbs to the incident photon energy of the solar cell.

Here, QE given as the ratio of bandgap energy of the material to the photon energy,

$$QE(E) = \frac{E}{E_p} \quad (3.3)$$

Here,

$E$  = Bandgap energy.

$E_p$  = Variable photon energy.

Energy is inversely related to the wavelength as,

$$E = \frac{hc}{\lambda} \quad (3.4)$$

So, wavelength becomes,

$$\lambda = \frac{hc}{E} \quad (3.5)$$

So, quantum **efficiency** as a function of wavelength ( $\lambda$ ) can be written as,

$$QE(\lambda) = \frac{\lambda_p}{\lambda} \quad (3.6)$$

Here,

$\lambda_p$  = Variable photon wavelength.

$\lambda$  = Wavelength of bandgap energy.

The short **circuit** current density can be found for the CNT and Si individually, from the ~~data~~ found for the terrestrial solar spectrum for AM 1.5, by integrating over appropriate range of wavelength.

### 3.4 J-V Characteristics

Total **current** density (J), load voltage (V) relationship can be expressed as,

$$J = J_{sc} - J_{dark}(V) \quad (3.7)$$

Here,  $J_{dark}(V)$  is the dark current density produced when load is present and a potential difference (V) develops across the terminals of the cell. This potential difference generates a current which acts in the opposite direction to the photocurrent, and the net current is reduced from its short circuit current.

For an **ideal** diode the dark current density varies like

$$(3.8)$$

Where,  $J_0$  is a constant known as reverse saturation current,  $k$  is Boltzmann's constant and  $T$  is temperature in Kelvin. Normally value of  $J_0$  is varied from  $10^{-10}$  mA/cm<sup>2</sup> to  $10^{-12}$  mA/cm<sup>2</sup> for a typical CNT-Si heterojunction solar cell [4]. We assumed  $10^{-10}$  mA/cm<sup>2</sup> for our calculation.

An equivalent circuit for a typical ideal solar cell can be shown as Figure 03.4.

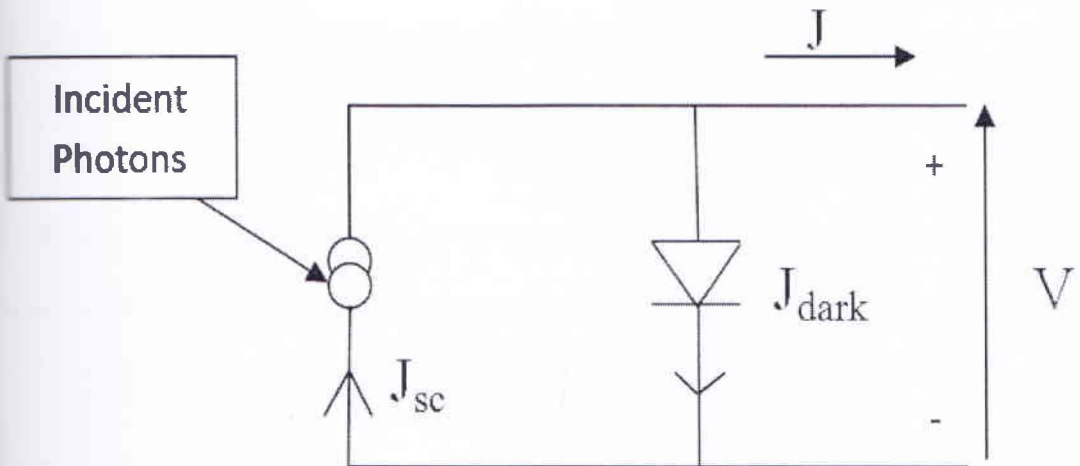


Figure 03.4: Equivalent circuit of ideal solar cell.

### 3.5 Open Circuit Voltage ( $V_{oc}$ )

When the contacts are isolated, the potential difference has its maximum value, which is known as open circuit voltage ( $V_{oc}$ ). This is equivalent to the condition when the dark current and short circuit photocurrent exactly cancel out. For the ideal diode,  $V_{oc}$  can be written as,

$$V_{oc} = \frac{k_B T}{q} \ln \left( \frac{J_{sc}}{J_0} + 1 \right) \quad (3.10)$$

Equation (3.10) shows that  $V_{oc}$  increases logarithmically with light intensity.

### 3.6 Efficiency

The operating region of the solar cell is in the range from 0 to  $V_{oc}$ , in which the cell delivers power. The power density of the cell is given by

$$P = JV \quad (3.11)$$

$P$  reaches a maximum at the cell's operating point or maximum power point. This occurs at some voltage  $V_m$  with a corresponding current density,  $J_m$  shown in Figure 03.5.

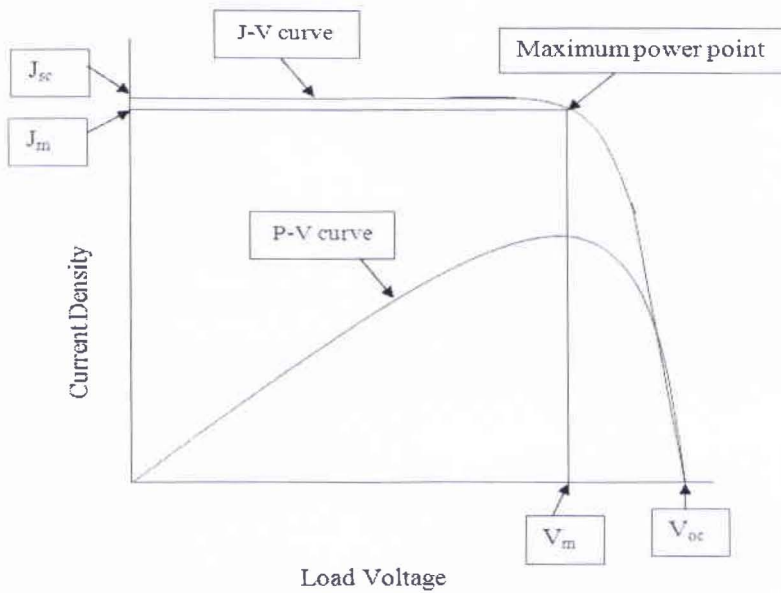


Figure 03.5: J-V and P-V curves showing  $V_{oc}$ ,  $J_{sc}$ , maximum power point,  $J_m$  and  $V_m$ .

Ratio of the maximum power from the solar cell to the product of  $V_{oc}$  and  $J_{sc}$  is known as fill factor (FF), graphically the FF is a measure of the "squareness" of the solar cell J-V curve and is also the area of the largest rectangle which will fit in the J-V curve. The FF is illustrated in Figure 03.5. FF is expressed as,

$$FF = \frac{J_m V_m}{J_{sc} V_{oc}} \quad (3.12)$$

For an ideal solar cell,  $FF=1$ .

Efficiency,  $\eta$  of solar cells is calculated as the ratio between the generated maximum power,  $P_m$  generated by a solar cell and the incident power,  $P_{in}$ .

The incident power is equal to the irradiance of AM1.5 spectrum, normalized to  $1000\text{W/m}^2$ .  $\eta$  is determined from the J-V curve (Figure 03.5) by following equation (3.12),

$$\eta = \frac{P_m}{P_{in}} = \frac{I_{sc}V_{oc}FF}{P_{in}} \quad (3.13)$$

The **irradiance** of AM1.5 spectrum can be calculated from the spectral power density,  $S(\lambda)$  by equation (3.13) from the data,

$$P_{in} = \int_0^{\infty} S(\lambda) d(\lambda) = \int_0^{\infty} F(\lambda)\lambda d(\lambda) \quad (3.14)$$

Equation (3.14) is for ideal case. We assumed 100% absorption of photons and no reflection.

These **four** quantities:  $J_{sc}$ ,  $V_{oc}$ , FF and  $\eta$  are the key performance characteristics of a solar cell, **which** are defined for particular illumination condition.



# CHAPTER 4

## Results and Discussion

Calculations have been made with the variation of CNT diameter from around 1nm to 2nm. The chirality of the CNT has been chosen such that it satisfies the semiconductive behavior of the CNT. Energy band diagrams, J-V characteristics and P-V characteristics of three devices are given by changing the diameter of the semiconducting CNT.

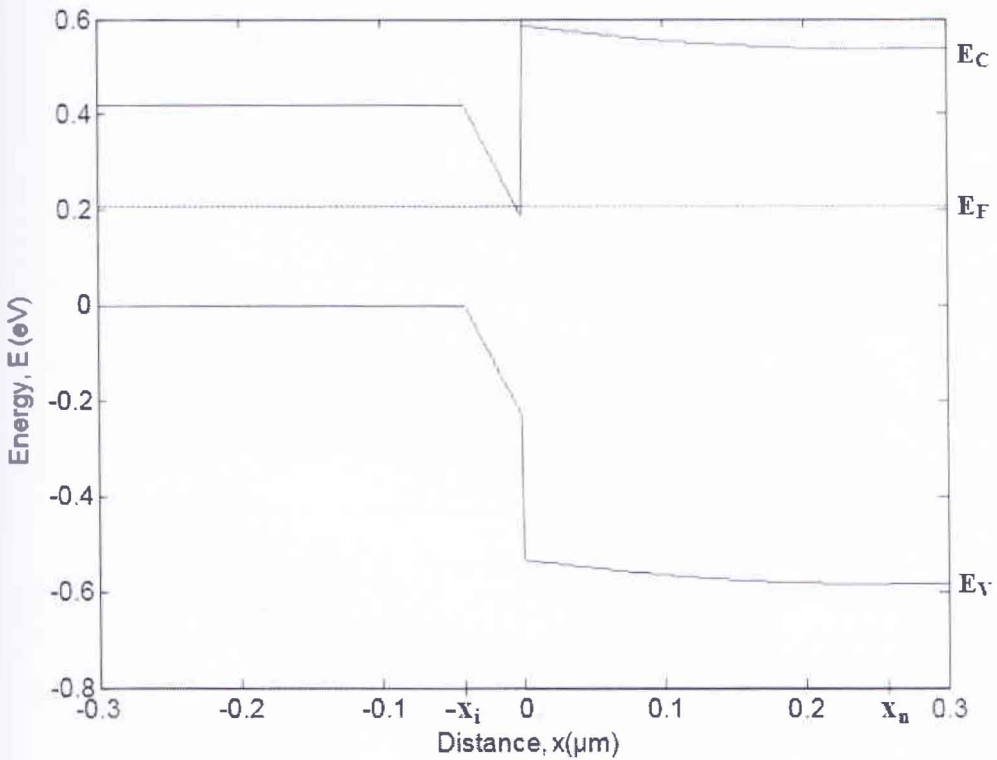


Figure 04.1: Energy band diagram of CNT-Si heterojunction for 1.92nm diameter of CNT.



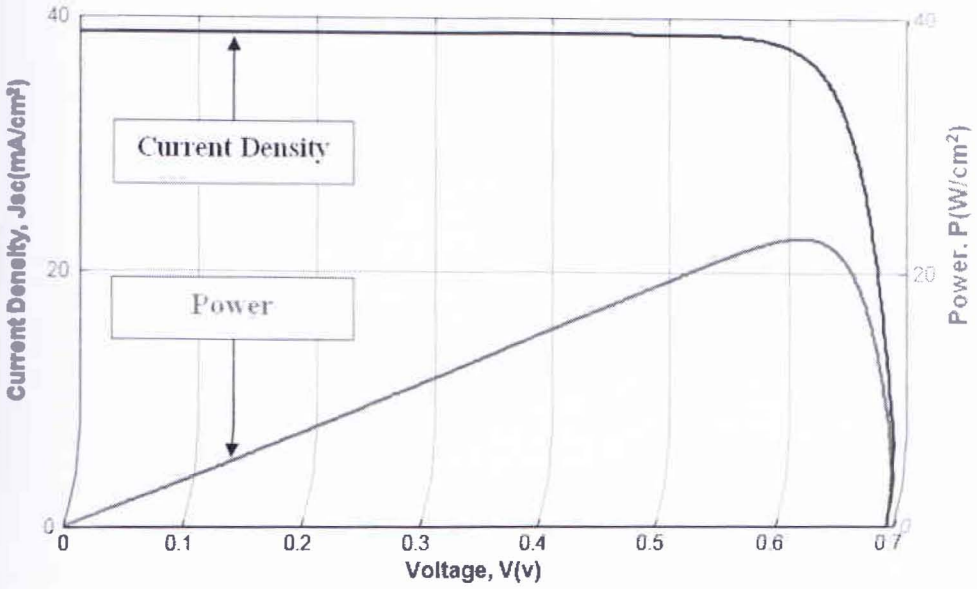


Figure 04.2: The J-V and P-V curves for 1.92nm diameter of CNT.

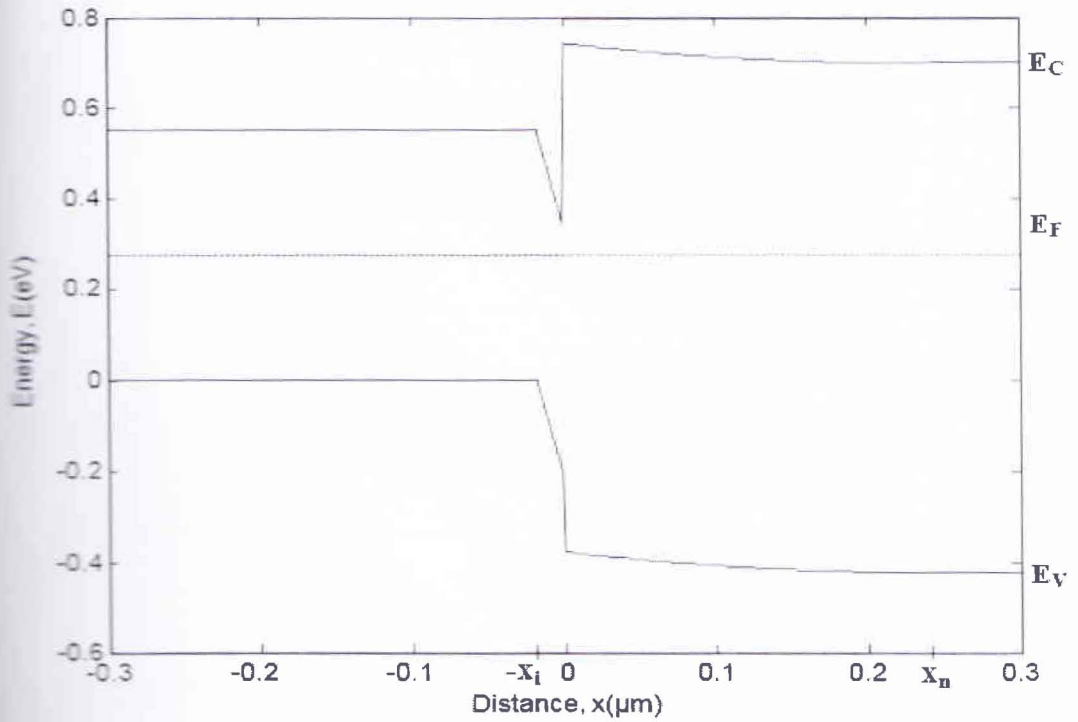


Figure 04.3: Energy band diagram of CNT-Si heterojunction for 1.45nm diameter of CNT.

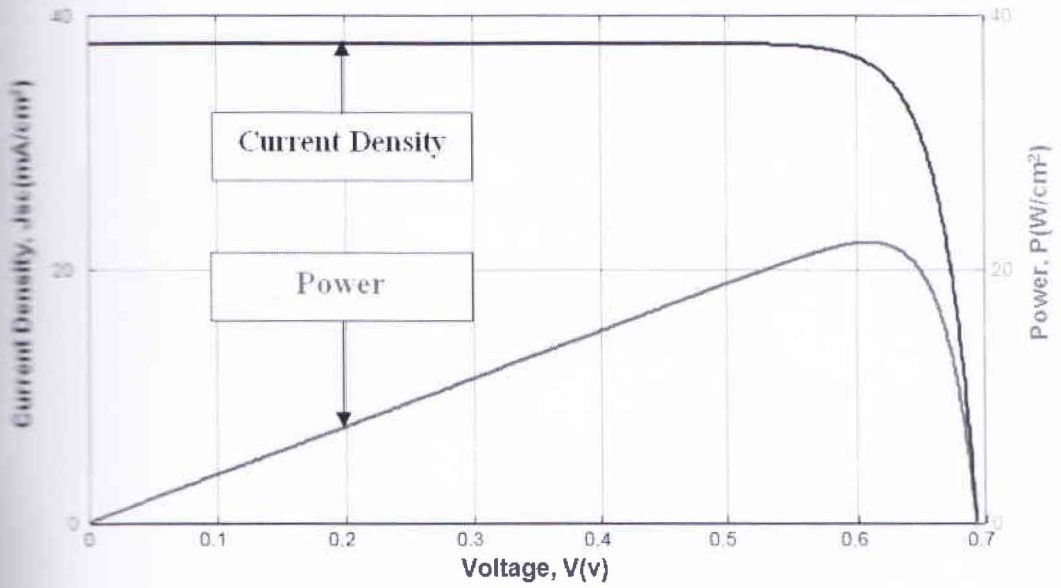


Figure 04.4: The J-V and P-V curves for 1.45nm diameter of CNT.

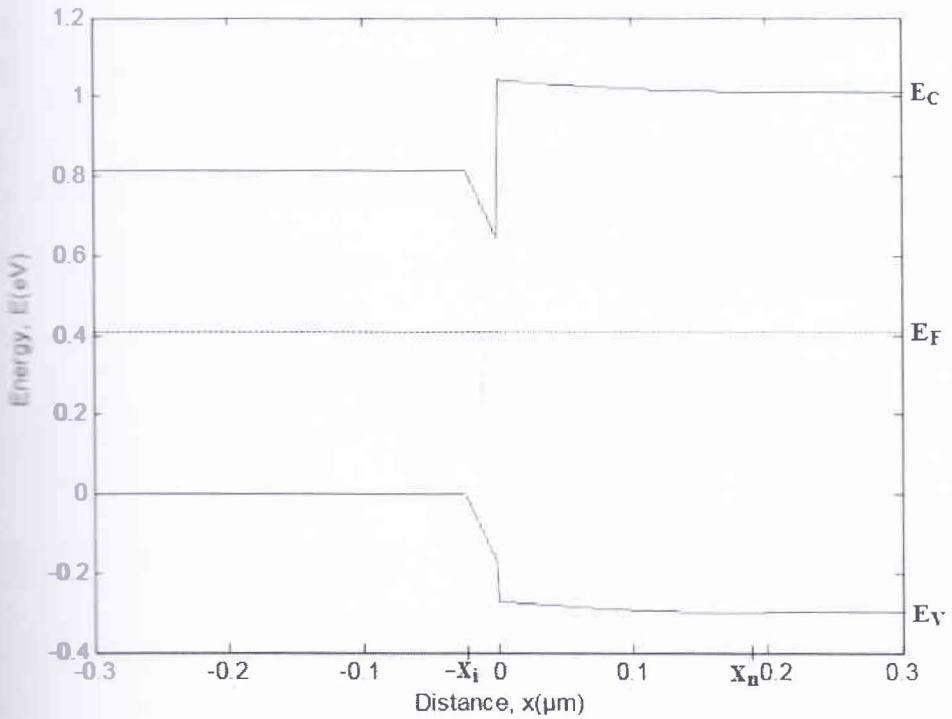


Figure 04.5: Energy band diagram of CNT-Si heterojunction for 0.98nm diameter of CNT.

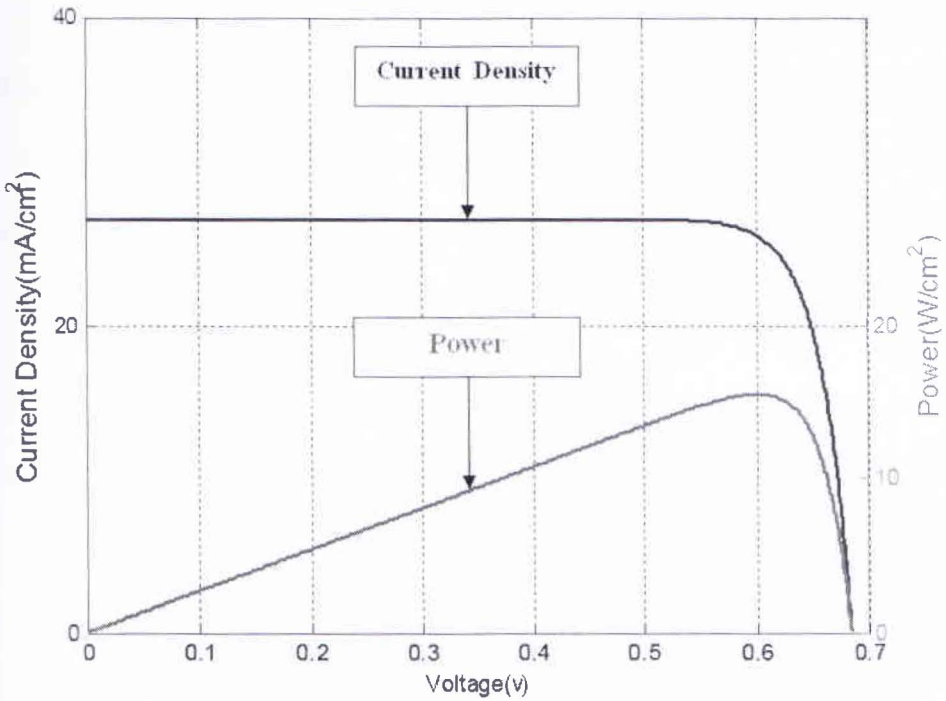


Figure 04.6: The J-V and P-V curves for 0.98nm diameter of CNT.

To plot the energy band diagrams we assumed that CNT as intrinsic semiconductor material and Si as n-type material. The bandgap of the semiconductive CNTs are calculated from the equation (4.1).

$$E_g = \frac{0.8}{d} \quad (4.1)$$

Where,  $E_g$  is the energy band gap of CNT in eV.

$d$  is the diameter of CNT in nanometer.

We have chosen the diameters of 1.92nm, 1.74nm, 1.6nm, 1.45nm, 1.32nm, 1.20nm, 1.12nm, 1.04nm, and 0.985nm. The energy bandgaps are found sequentially for the chosen diameters as 0.417eV, 0.460eV, 0.500eV, 0.553eV, 0.610eV, 0.668eV, 0.713eV, 0.771eV, 0.812eV respectively. The band diagrams shows that  $\Delta E_c$  remains constant for all diameters because electron affinity ( $\chi$ ) is constant for the CNT which is, 4.45eV and for Si 4.05eV.

Terrestrial solar irradiation for AM1.5G with irradiance  $100\text{mW}/\text{cm}^2$  data is used to calculate the short circuit current density,  $J_{sc}$ . To calculate  $J_{sc}$ , we assumed a range of photon energy which is divided in two regions. First region is the energy equals to bandgap of the CNT to energy equals to bandgap of the Si (1.12eV) as shown in Figure 03.3. CNT absorbs the photon energy in this range.

Second region is the energy equals to the bandgap of the Silicon,  $E_g(\text{Si})$  to  $E_g(\text{Si}) + 1.5K_B T$  as shown in Figure 03.3. Silicon (Si) absorbs the photon energy in this range.

Total current density,  $J_{sc}$  and open circuit voltage,  $V_{oc}$  found with the variation of the CNT diameter by using equations (3.1) and (3.10) is given in Table 01.



CNT diameter(nm)	Short Circuit Current Density, $J_{sc}$ (mA/cm <sup>2</sup> )			Open Circuit Voltage, $V_{oc}$ (Voltage)
	$J_{sc(cnt)}$ (mA/cm <sup>2</sup> )	$J_{sc(Si)}$ (mA/cm <sup>2</sup> )	$J_{sc} = J_{sc(cnt)} + J_{sc(Si)}$ (mA/cm <sup>2</sup> )	
1.92	24.4459	14.2688	38.7148	0.6937
1.74	24.4107	14.2688	38.6795	0.6937
1.60	24.3988	14.2688	38.6676	0.6937
1.45	23.4469	14.2688	37.7158	0.6931
1.32	22.2269	14.2688	36.4957	0.6922
1.20	21.9186	14.2688	36.1874	0.6920
1.12	21.5671	14.2688	35.8359	0.6917
1.04	16.7665	14.2688	31.0353	0.6880
0.98	12.6241	14.2688	26.8929	0.6843

**Table 01:** The current density and open circuit voltage with different diameters of CNT.

The result (Table 01) shows that the short circuit current density decreases with the decrement of the diameter of the CNT. Open circuit voltage is slightly decreased with the decrement of the CNT diameter. But there is no change in the short circuit current of n-side (Si) because the bandgap of p-side is unchanged.

The Fill Factor ( $FF$ ) and the efficiency ( $\eta$ ) are also calculated by using equation (3.12) and (3.13) with the variation of the diameter of the CNT.

Here total input power,  $P_{in} = 100\text{mW/cm}^2$ . Result is shown in the Table 02

CNT diameter(nm)	Maximum power point density, $P_{mp}$ ( $\text{w/cm}^2$ )	Voltage at maximum power point, $V_{mp}$ (V)	Current density at maximum power point, $J_{mp}$ ( $\text{mA/cm}^2$ )	Fill Factor, $FF$ (in %)	Efficiency, $\eta$ (in %)
1.92	22.67	0.6076	37.30	84.387	22.663
1.74	22.65	0.6076	37.27	84.396	22.645
1.60	22.64	0.6076	37.26	84.399	22.639
1.45	22.06	0.6070	36.34	84.383	22.580
1.32	21.32	0.6070	35.12	85.129	21.506
1.20	21.13	0.6061	34.86	84.379	21.129
1.12	20.92	0.6066	34.48	84.374	20.914
1.04	18	0.6012	29.93	84.272	17.993
0.98	15.51	0.6007	25.81	84.248	15.504

Table 02: The  $P_{mp}$ ,  $V_{mp}$ ,  $J_{mp}$ ,  $FF$  and  $\eta$  with different diameters of CNT.

From the above result (Table 02) it can be said that the maximum power point density and the short circuit current density at maximum power point decreases with the decrement of the diameter of the CNT. The voltage at maximum power point is slightly

changed with changing CNT diameter. But it is negligible for all practical purposes. Fill factor and efficiency also decreases with the decrement of the CNT diameter.

The efficiency is almost constant and maximum from around 1.5nm to 2nm diameter of CNT which is shown in figure 04.7. Then the efficiency decreases with decrement of the diameter of CNT as shown in figure 04.7. So diameter of CNT from 1.5nm to 2nm is best for our CNT-Si heterojunction solar cells.

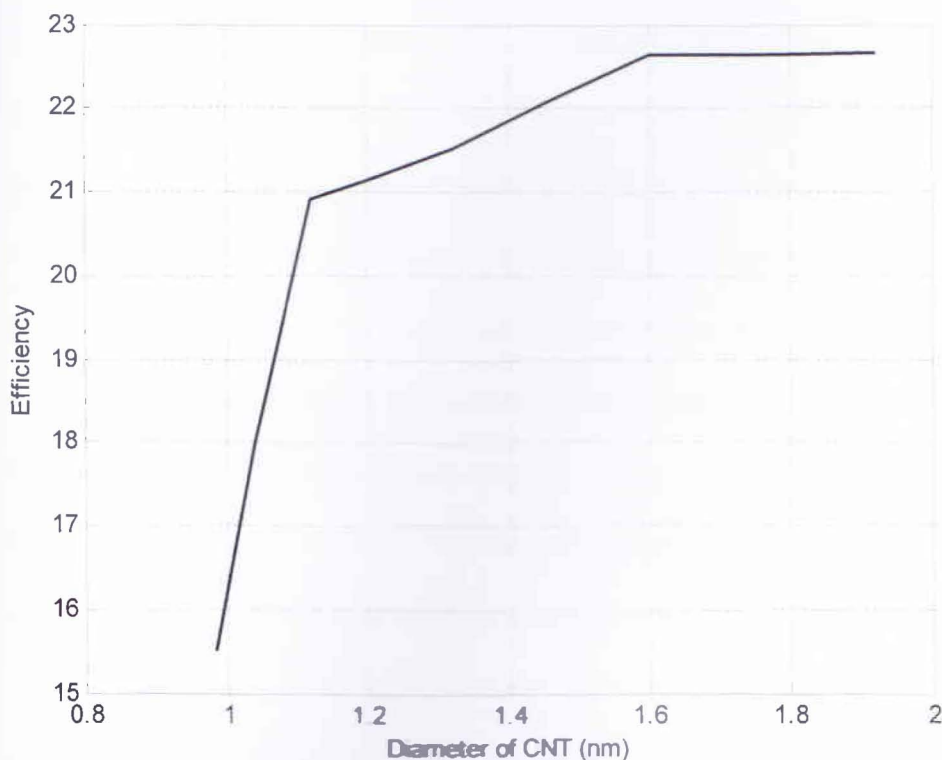


Figure 04.7: The plot of diameter of CNT vs efficiency.

# CHAPTER 5

## Conclusions

### 5.1 Summary

In our work we have studied the CNT-Si heterojunction solar cells. We have analyzed the band diagram of CNT-Si Heterojunction using the parameters of the CNT. For this model we assumed CNT as intrinsic semiconductor material and Si as n-type material. The band bending of intrinsic region was unknown to us. We assumed the band bending of intrinsic CNT to be linear and developed an equation to plot the band diagram of i-n heterojunction. To observe the band diagram of CNT-Si heterojunction for different diameters of semiconducting CNT, we have shown the band diagram for CNT diameter of 1.92nm, 1.45nm and 0.98nm. We have also calculated the solar cell parameters for the different diameters of the CNT. To calculate the solar cell parameters we have used the terrestrial irradiance data for AM1.5 with average input power density of  $100\text{mWcm}^{-2}$ . We have included Quantum efficiency to calculate the short circuit current density. To find the current density in CNT side we have assumed that CNT can absorb photon have energy ranges from energy equals to CNT bandgap to Si bandgap and integrated over these region. And Si can absorb the photon have energy ranges from Si bandgap energy,  $E_g(\text{Si})$  to  $E_g(\text{Si})+1.5K_B T$  and again integrated over this region to find the current density at Si. Then we compared the calculated result for varying 1nm-2nm of the CNT diameter and found that with the decrements of the CNT diameter total current density also decreases. In FF slight change has been observed and efficiency is also decreased with the CNT diameter. Efficiency remains almost about 23% for the CNT diameter 1.92nm,



1.74nm, 1.60nm, and 1.45nm. Then efficiency decreases notably with the decrement of the CNT diameter. So we can conclude that the solar cell will be more efficient if the diameter of CNT is chosen around the 2nm.

## **5.2 Suggestion for future work**

In our work we have make some assumptions to make our calculation easy. To calculate the band bending of the intrinsic CNT we have assumed that band bending is linear. In future actual band bending of the intrinsic CNT can be analyzed to determine more appropriate band diagram of CNT-Si heterojunction. We studied i-n CNT-Si heterojunction solar cell instead of p-n heterojunction solar cell. In future p-n heterojunction solar cells can be studied. In CNT region of the heterojunction a quantum well has been introduced which confines the electrons. We did not consider the quantum mechanical effect of that region. In future quantum mechanical effect can be introduced to understand the behavior of confined electron in the quantum well of CNT region. We have assumed that all electron hole pair generated by the light contributes to the current generation and neglected the recombination of electrons. In future recombination of electron can be included to calculate the total current. To analyze J-V characteristics of the solar cell, we have assumed that there is small impact of biasing effect of the bias voltage in CNT-Si heterojunction and built in potential remains constant. In future biasing effect can also be included in the calculation of J-V characteristics of the solar cells. All of our calculations are made by assuming that solar cell is ideal and we didn't introduce the effect of series and shunt resistance in the load side. In future this resistive effect can be included to analyze the non ideal heterojunction solar cells.

## References

- [1]. S.Subash and Masud H Chowdhury, “High Efficiency Carbon Nanotube Based Solar Cells for Electronics Devices”, *Appears in IEEE 12<sup>th</sup> International Symposium on Integrated circuits*, 131-140 (2009).
- [2]. M.A.Green, “Photovoltaic principles” Vol.-14, 11-17 (2002).
- [3]. Jinquan Wei, Yi Jia, Qinke Shu, Zhiyi Gu, Kunlin Wang, daming Zhuang, Gong Zhang, Zhicheng Wang, Jianbin Luo, Anyuan Cao and Dehai Wu, “Double-Walled Carbon Nanotube Solar Cells”, *Nano Lett.*, Vol.-7, 2317-2321 (2007).
- [4]. Yi Jia, Jinquan Wei, Kunlin Wang, Anyuan Cao, Qinke Shu, Xuchun Gui, Yanqiu Zhu, Daming Zhuang, Gong Zhang, Beibei Ma, Liduo Wang, Wenjin Liu, Zhicheng Wang, Jianbin Luo, and Dehai Wu., “Nanotube-Silicon Heterojunction Solar Cells”, *Advanced Materials*, Vol.-20, 4595-4598 (2008).
- [5]. Z. Li, V. P. Kunets, V. Saini, Y. Xu, E. Dervishi, G. J. Salamo, and A. R. Biris, “SOCl<sub>2</sub> enhanced photovoltaic conversion of single wall carbon nanotube/*n*-silicon heterojunctions”. *Appl. Phys. Lett.* Vol.-93, 243117-243121 (2008).
- [6]. P.L.Ong, W.B.Euler, I.A.Levitsky, “Hybrid Solar Cells Based On Single-walled Carbon Nanotubes/Si Heterojunctions”, *Nanotechnology*, Vol.-10, 957-961 (2010).

- [7]. Y.F.Zhang, Y.F.Wang, N.Chen, Y.Y.Wang, Y.Z.Zhang, Z.H.Zhou and L.M. Wei, “Photovoltaic enhancement of Si solar cells by assembled carbon nanotube”, *Nano-Micro Lett.*, Vol.-2, 22-25 (2010).
- [8]. Yi Jia, Anyuan Cao, Xi Bai, Zhen Li, Luhui Zhang, Ning guo, Jinquan Wei, Kunlin Wang, Hongwei Zhu, Dehai Wu, and P. M. Ajayan, “ Achieving High Efficiency Silicon-Carbon Nanotube Heterojunction Solar Cells by Acid Doping”, *Nano Lett.*, Vol.-11,1901-1905 (2011).
- [9]. H.Zhou, H.E.Unalan, P.Hiralal, A. Colli, S.C.Tan, L.Wang, F.Kong, G.Aamaratunga, “Heterojunction photovoltaic Devices Utilizing Single Wall Carbon Nanotube Thin Films and Silicon Substrates”, *23<sup>rd</sup> IEEE Photovoltaic Specialists Conference*, 1-5 (2008).
- [10]. Jenny Nelson, “The physics of solar cells”, Imperial College press, UK, 276 (2003).
- [11]. Donald A. Neamann, ”Semiconductor Devices and Physics”, The McGraw-Hill Companies, Inc., New York, 601, (2003).



# ACKNOWLEDGEMENTS

We would like to thank Dr. Anisul Haque, Professor and Chairperson, Department of Electrical and Electronic Engineering (EEE), East West University (EWU), Dhaka, our supervisor, for his constant guidance, supervision, constructive suggestion and constant support during this thesis.

We are grateful to Dr. Khairul Alam, Associate professor Department of EEE, EWU and Mr. Mahmudur Rahman Siddiqui, Research Lecturer, Department of EEE, EWU, for their suggestions and help.

We also want to thank our parents and all of our friends for their moral support and helpful discussion during this work.



EWU, Dhaka

Authors

August, 2011